Conglobatins B–E: cytotoxic analogues of the C_2-symmetric macrodiolide conglobatin

Heather J. Lacey[1,2*], Thomas J. Booth[3], Daniel Vuong[1], Peter Rutledge[2], Ernest Lacey[1,4], Yit-Heng Chooi[3] and Andrew M. Piggott[4]

[1] *Microbial Screening Technologies, Smithfield, Sydney, NSW 2164, Australia*

[2] *School of Chemistry, The University of Sydney, Camperdown, Sydney, NSW 2006, Australia*

[3] *School of Molecular Sciences, The University of Western Australia, Crawley, Perth, WA 6009, Australia*

[4] *Department of Molecular Sciences, Macquarie University, North Ryde, Sydney, NSW 2109, Australia*

Abstract

Chemical investigation of a previously unreported indigenous Australian *Streptomyces* strain MST-91080 has identified six novel analogues related to the oxazole-pendanted macrodiolide, conglobatin. Phylogenetic analysis of the 16S rRNA gene sequence identified MST-91080 as a species of *Streptomyces*, distinct from reported conglobatin producer, *S. conglobatus* ATCC 31005. Conglobatins B – E diverge from conglobatin through differing patterns of methylation on the macrodiolide skeleton. The altered methyl positions suggest a deviation from the published biosynthetic pathway, which proposed three successive methylmalonyl-CoA extender unit additions to the conglobatin monomer. Conglobatins B1, C1 and C2 exhibited more potent cytotoxic activity selectively against the NS-1 myeloma cell line (IC_{50} 0.084, 1.05 and 0.45 µg ml^{-1}, respectively) compared to conglobatin (IC_{50} 1.39 µg ml^{-1}).

Streptomyces/conglobatin/macrodiolide/oxazole/cytotoxic

Introduction

Macrocyclic lactones represent a mainstay of drug discovery from microbes since the discovery of the first macrocycle natural product, pikromycin in 1950 [1]. In the 70 years since, over 6,000 macrolide natural products have been reported [2]. Within the structural diversity of macrolides, some 13% are macrodiolides with symmetrical and asymmetrical arrangements of a second ester in the macrocycle. It is therefore curious that 16-membered macrolides are represented by only a handful of symmetric 16-membered macrodiolides drawn from across nature. Only a single plant metabolite, chaksine, from the legume *Cassia absus* [3], a single lichen metabolite, lepranthin, from *Arthonia impolita* [4], and a single family of 12 analogues belonging to the pyrenophorin class [5], including the vermiculins [6] and trichobotryside A [7], have been reported from diverse range of endophytic and plant pathogenic fungi. Within actinomycetes, only two groups of 16-membered macrodiolides bearing a symmetrical disposition of lactones have been reported from *Streptomyces* species: a family of 16-membered diene-conjugated lactones, the elaiophylins (including halichoblelides, efomycins and SNA 4606-1) first described by Kaiser and Keller-Schierlein in 1981 [8] and subsequently by others [9-12], and a single conjugated α,β unsaturated lactone, conglobatin (**1**), reported by researchers at Roche in 1979 [13]. The discovery of **1** was driven by its abundance as a co-metabolite of the ionophore ionomycin, discovered some years earlier in *Streptomyces conglobatus* ATCC 31005 [13]. Despite the absence of biological activity against fungi, bacteria, protozoa and mammalian cells presented in the original report, subsequent *in vitro* studies have revealed that conglobatin has cytotoxic, antitrypanosomal and antimalarial activities [14-16].

Structurally, **1** is C_2-symmetric, bearing pendant 5-substituted oxazole moieties. The two α,β-unsaturated lactones are the dominant chromophores, providing a distinct single UV maximum at 214 nm. In 2015, the conglobatin (*cong*) biosynthetic gene cluster (BGC) was reported [17]. Biosynthesis of 1 is mediated by a nonribosomal peptide synthetase (NRPS)-like loading module (encoded by *congA*) coupled to four polyketide synthase (PKS) modules (encoded by *congBCD*), and a cyclodehydratase (encoded by *congE*). During biosynthesis, an oxazole-containing diketide is generated by the subsequent formylation, cyclisation and extension of a glycine starter unit through coordinated action of CongABE. Three additional Claisen condensations yield a pentaketide that forms mature **1** following head-to-tail dimerization catalysed by the thioesterase domain of CongD. Notably, the acetyltransferase domain of module three in the PKS is mutated, leading to module 'stuttering' and the incorporation of three methylmalonyl extender units, resulting in the characteristic 2,4,6-trimethylated pattern of **1** [17].

As part of our continuing search for chemical diversity from Australian microbes [18-20], we constructed a library of 50,000 talented microbes, each containing high levels of secondary metabolites and a diverse array of UV spectra. The library, which was drawn from 500,000 microbes sampled from 25,000 soil, marine and plant samples collected across the length and breadth of Australia, represents a unique continental bioresource. From this collection, an unusual soil actinomycete, *Streptomyces* sp. MST-91080 with a unique secondary metabolite profile, was obtained from Yeppoon, Queensland, Australia. Notably, MST-91080 exhibited a highly characteristic family of metabolites displaying a single UV maximum at 214 nm consistent with the presence of an α,β-unsaturated carbonyl moiety as found in conglobatin and related compounds. Herein, we report the isolation, structural elucidation and bioactivity

profiling of this dominant metabolite class, leading to the discovery of six novel conglobatin analogues, conglobatins B1 (**2**), C1 (**3**), C2 (**4**), D1 (**5**), D2 (**6**) and E (**7**), together with conglobatin (**1**) itself.

Methods and Materials

General

NMR spectra were acquired in DMSO-d_6 on a Bruker Avance II DRX-600K 600 MHz spectrometer at 25 °C. NMR spectra were processed using Topspin 3.5 and referenced to the residual solvent signals (DMSO-d_6; δ_H 2.49 / δ_C 39.5). High resolution electrospray ionisation mass spectra (HRESIMS) were acquired by direct infusion in MeCN on either a Bruker Apex Qe 7T Fourier Transform Ion Cyclotron Resonance mass spectrometer equipped with an Apollo II ESI/MALDI dual source or a Q Exactive Plus hybrid quadrupole-Orbitrap mass spectrometer. Electrospray ionisation (ESI) mass spectrometry was carried out with an Agilent 1260 Infinity HPLC series equipped with an Agilent 6120 Infinity series mass detector in both positive and negative ion modes. All HPLC and LC-MS data were analysed with in-house software COMET [21], respectively. Chiroptical measurements were acquired in MeOH with a Perkin-Elmer Model 341 polarimeter in a 50 × 5 mm cell. UV-vis spectra were acquired in MeCN on a Varian Cary 4000 spectrophotometer between 200 – 600 nm with a cell size of 10 × 10 mm. FT-IR spectra were obtained with Bruker Platinum-ATR and processed with OPUS software.

Analytical HPLC was performed on a gradient Agilent 1260 Infinity quaternary HPLC system. The column was an Agilent Zorbax SB-C_{18} (2.1 × 50 mm, 1.8 μm) eluted with a 0.6 ml min^{-1} gradient of 10-100% MeCN/H_2O (0.01% TFA) over 8.33 min. Preparative HPLC was performed on a gradient Shimadzu HPLC system comprising of two LC-8 preparative liquid pumps with static mixer, SPD-M10AVP diode array detector and SCL-10AVP system controller with standard Rheodyne injection port. The columns used in the purification of the metabolites were selected from either a Vydac C_{18} column (50 × 100 mm, 5 μm; Grace Discovery), a Zorbax SB-C_{18} column (50 × 150 mm, 5 μm; Agilent) or an Alltima C_{18} (22 × 250 mm, 5 μm, Grace Discovery) isocratically with MeCN/H_2O mixtures containing 0.01% TFA modifier.

Taxonomic studies

Genomic DNA from *Streptomyces* sp. MST-91080 and *Streptomyces conglobatus* was extracted using E.Z.N.A. Bacterial DNA Kit (Omega Bio-Tek) following the manufacturers protocol. 16S rRNA was amplified via PCR using the primers S-D-Bact-0341-b-S-17 (CCTACGGGNGGCWGCAG) and S-D-Bact-0785-a-A-21 (GACTACHVGGGTATCTAATCC) [22] and sequenced using the AGRF Sanger sequencing platform (Melbourne, Australia). Sequences were submitted to GenBank under accessions MT013375 (MST-91080) and MT013374 (ATCC 31005). Non-redundant sequences were aligned using Clustal Omega [23] along with representative *Streptomyces* spp. 16S sequences identified from Labeda et al., 2012 [24]. A phylogenetic tree was generated using FastTree 2 [25] using default setting and visualised in iTOL [26] (Supplementary Information Figure S61).

Fermentation and extraction

MST-91080 was cultured on ISP2 agar plates for seven days at 28 °C. A spore suspension (H_2O; 100 ml) was used to inoculate pearl barley (3.5 kg), which was incubated for seven days at 28 °C. The fermentation was extracted with acetone (2 × 1800 ml) and the acetone layer was filtered and concentrated by evaporation to an aqueous slurry (1000 ml) before being partitioned against ethyl acetate (2 × 1200 ml). The ethyl acetate fraction was evaporated to dryness, then redissolved in methanol (200 ml) and re-partitioned against hexane (2 × 400 ml) to obtain a methanolic crude extract.

Isolation of compounds

After *in vacuo* reduction, the crude (3.2 g) was dissolved in chloroform and applied to a silica gel column (80 g) and eluted with a stepwise gradient of 0–100% MeOH in $CHCl_3$, collecting a total of twelve fractions (500 ml). The metabolites sharing a common UV_{max} of 214 nm eluted in fractions 4 (475 mg) and 5 (197 mg), which were combined. Fraction 4/5 was dissolved in MeOH (4 ml) and was further fractionated by preparative HPLC (Hypersil C_{18}, isocratic 70% MeCN/H_2O containing 0.01% TFA, 60 ml min^{-1}). The conglobatin compounds eluted in fractions A3 (11.2 mg), A4 (199.2 mg), A5 (126.7 mg) and A7 (25.6 mg). Fraction A3 was further resolved by preparative HPLC (Hypersil C_{18}, isocratic 60% MeCN/H_2O containing 0.01% TFA, 20 ml min^{-1}), yielding **6** (t_R= 11.9 min, 1.1 mg) and **7** (t_R= 12.5 min, 1.5 mg). Fraction A4 was dissolved in MeOH (3 ml) and fractionated (Hypersil C_{18}, isocratic 60% MeCN/H_2O containing 0.01% TFA, 20 ml min^{-1}) in three consecutive separations, yielding **5** (t_R= 14.1 min, 25.3 mg) and **3** (t_R= 15.6 min, 36.3 mg). While A5 was resolved by preparative HPLC (Hypersil C_{18}, isocratic 67.5% MeCN/H_2O containing 0.01% TFA, 20 ml min^{-1}), to yield **4** (t_R= 14.4 min, 3.8 mg) and **2** (t_R= 15.4 min, 73.4 mg). Finally, the most non-polar fraction A7 was fractionated by preparative HPLC (Hypersil C_{18}, isocratic 80% MeCN/H_2O containing 0.01% TFA, 20 ml min^{-1}) in two separations to provide **1** (t_R= 10.1 min, 6.03 mg).

Characterisation of metabolites

Conglobatin B1 (**2**): white powder; m.p. 98 – 100 °C; $[\alpha]_D^{20}$ –45 (*c* 0.03, MeOH); UV (MeCN) λ_{max} (log ε) 214 (4.46) nm; IR (ATR) ν_{max} 3123, 2959, 2927, 2871, 1698, 1271, 1098, 745, 646 cm^{-1}; HRESI(+)MS *m/z* 485.2490; calcd. for $C_{27}H_{37}N_2O_6^+$ $[M + H]^+$, 485.2646.

Conglobatin C1 (**3**): white powder; m.p. 138 – 140 °C; $[\alpha]_D^{20}$ –55 (*c* 0.05, MeOH); UV (MeCN) λ_{max} (log ε) 214 (4.42) nm; IR (ATR) ν_{max} 3101, 2939, 2867, 1698, 1274, 1098, 973, 651 cm^{-1}; HRESI(+)MS *m/z* 471.2490; calcd. for $C_{26}H_{35}N_2O_6^+$ $[M + H]^+$, 471.2490.

Conglobatin C2 (**4**): white powder; $[\alpha]_D^{20}$ –25 (*c* 0.03, MeOH); UV (MeCN) λ_{max} (log ε) 214 (4.67) nm; HRESI(+)MS *m/z* 471.2482; calcd. for $C_{26}H_{35}N_2O_6^+$ $[M + H]^+$, 471.2490.

Conglobatin D1 (**5**): white solid; $[\alpha]_D^{20}$ –11 (*c* 0.03, MeOH); UV (MeCN) λ_{max} (log ε) 214 (4.50) nm; m.p. 98 – 100 °C; IR (ATR) ν_{max} 3139, 2935, 2864, 1705, 1653, 1608, 1512, 1273, 1099, 828, 748, 645 cm^{-1}; HRESI(+)MS *m/z* 457.2327; calcd. for $C_{25}H_{33}N_2O_6^+$ $[M + H]^+$, 457.2333.

Conglobatin D2 (**6**): colourless oil; $[\alpha]_D^{20}$ –46 (*c* 0.01, MeOH); UV (MeCN) λ_{max} (log ε) 200 (4.69) nm; HRESI(+)MS *m/z* 457.2322; calcd. for $C_{25}H_{33}N_2O_6^+$ $[M + H]^+$, 457.2333.

Conglobatin E (**7**): colourless oil; $[\alpha]_D^{20}$ –27 (*c* 0.01, MeOH); UV (MeCN) λ_{max} (log ε) 214 (4.39) nm; HRESI(+)MS *m/z* 443.2172; calcd. for $C_{24}H_{31}N_2O_6^+$ $[M + H]^+$, 443.2177.

Biological assays

NS-1 (ATCC TIB-18) mouse myeloma cells and NFF (ATCC PCS-201) human fibroblast cells were inoculated in 96-well microtitre plates (190 µl) at 50,000 cells ml^{-1} in DMEM (Dulbecco's Modified Eagle Medium + 10% fetal bovine serum (FBS) + 1% penicillin/streptomycin (Life Technologies)) and incubated in 37 °C (5% CO_2) incubator. At 48 h, resazurin (120 µg ml^{-1}; 10 µl) was added to each well and the plates were incubated for a further 48 h. Finally, the absorbance of each well at 605 nm was measured using a Spectromax plate reader (Molecular Devices). The absorbance measured using Spectromax plate reader (Molecular Devices) at 605 nm and the IC_{50} values determined using a sigmoidal dose response model with variable slope in Graphpad Prism 8.

Bacillus subtilis (ATCC 6633) and *Escherichia coli* (ATCC 25922) were used as indicative species for Gram-positive and Gram-negative antibacterial activity, respectively. A bacterial suspension (50 ml in 250-ml flask) was prepared in nutrient media by cultivation for 24 h at 250 rpm, 28 °C. The suspension was diluted to an absorbance of 0.01 absorbance units per ml, and 10 µl aliquots were added to the wells of a 96-well microtitre plate, which contained the test compounds dispersed in nutrient agar (Amyl) with resazurin (120 µg ml^{-1}). The plates were incubated at 28 °C for 48 h during which time the positive control wells changed colour from a blue to light pink colour. MIC end points were determined visually. The absorbance measured using Spectromax plate reader (Molecular Devices) at 605 nm and the IC_{50} values determined using a sigmoidal dose response model with variable slope in Graphpad Prism 8.

Candida albicans (ATCC 10231) was used as indicative species for antifungal activity. A yeast suspension (50 ml in 250 ml flask) was prepared in 1% malt extract broth by cultivation for 24 h at 250 rpm, 24 °C. The suspension was diluted to an absorbance of 0.005 and 0.03 absorbance units per ml for *C. albicans*. Aliquots (20 µl and 30 µl) of *C. albicans* was applied to the wells of a 96-well microtitre plate, which contained the test compounds dispersed in malt extract agar containing resazurin (120 µg ml^{-1}). The plates were incubated at 24 °C for 48 h during which time the positive control wells change colour from a blue to yellow colour. MIC end points were determined visually. The absorbance measured using Spectromax plate reader (Molecular Devices) at 620 nm and the IC_{50} determined using a sigmoidal dose response model with variable slope in Graphpad Prism 8.

Tritrichomonas foetus (strain KV-1) was used as an indicative species for antiprotozoal activity. *T. foetus* was inoculated in 96-well microtitre plates (200 µl) at 4×10^4 cells ml^{-1} in *T. foetus* medium (0.2% tryptone, Oxoid; 0.1% yeast extract, Difco; 0.25% glucose; 0.1% L-cysteine; 0.1% K_2HPO_4; 0.1% KH_2PO_4; 0.1% ascorbic acid; 0.01% $FeSO_4 \cdot 7H_2O$; 1% penicillin/streptomycin (10,000 U ml^{-1} / 10,000 µg ml^{-1}, Life Technologies Cat. No. 15140122), 10% new born calf serum (NBCS), Life Technologies). The plates were incubated in anaerobic jars (Oxoid AG25) containing Anaerogen satchel (Oxoid AN25) in 37 °C (5% CO_2) incubator. At 72 h, *T. foetus* proliferation was counted and % inhibition graphed to determine the IC_{50} values using a sigmoidal dose response model with variable slope in Graphpad Prism 8.

Giardia duodenalis (strain 713) were inoculated in 96-well microtitre plates (200 µl) at 4×10^5 cells/ml in Giardia medium (0.2% tryptone, Oxoid; 0.1% yeast extract, Difco; 0.5% glucose; 0.106% L-Arginine; 0.1% L-cysteine; 0.2% NaCl; 0.1% K_2HPO_4; 0.06% KH_2PO_4; 0.02% ascorbic acid; 0.0023% ferric ammonium citrate; 0.01% Bile (Sigma); 1% penicillin/streptomycin (10,000 U ml^{-1} / 10,000 µg ml^{-1}, Life Technologies Cat. No. 15140122), 10% newborn calf serum (NBCS), Life Technologies). The plates were incubated in anaerobic jars (Oxoid AG25) containing Anaerogen satchel (Oxoid AN25) in 37 °C (5% CO_2) incubator. At 96 h, *G. duodenalis* proliferation was counted and % Inhibition graphed to determine the IC_{50} values.

Eragrostis tef (teff) seed was used as indicative species for herbicidal discovery. 10 to 15 teff seeds were dispensed using LabTIE seed dispenser into the wells of a 96-well microtitre plate, which contained the test compounds dispersed in 200 µl of agar (1% w/v) per well. The plates were placed in a tray wrapped with semi-opaque bag, exposed to 1600 lux (inside the bag) using Power-Glo (20 W) and Sun-Glo (20 W) tubes, and incubated for 72 h at 24 °C and the inhibition of germination determined visually.

Results and Discussion

Taxonomy of the producing organism

MST-91080 was isolated from a sample collected from the topsoil in a public park located close to the Pacific Ocean coastline in the township of Yeppoon, Queensland, Australia in 1996. Sequences were queried against the NCBI BLAST nucleotide collection to identify closely related strains. The 16S rRNA gene sequence indicated that the strain is closely related to *Streptomyces albulus* strains NBRC 13410 and IMC S-0802 (100% sequence similarity) [27], *Streptomyces noursei* NBRC 15452 (100% sequence similarity) [28] and *Streptomyces palmae* CMU-AB204 (100% sequence similarity) [29].

Structural determination of isolated compounds

HRESI(+)MS analysis of conglobatin B1 (**2**) indicated a molecular formula $C_{27}H_{36}N_2O_6$ ($[M + H]^+$ *m/z* 485.2490, Δmmu –0.3) containing one carbon and two hydrogen atoms fewer than **1**. Similarly to **1**, the UV spectrum of **2** revealed a distinct maximum at 214 nm (Figure S52). The ^{13}C NMR spectrum of **2** (Table 1, Figure S9) revealed 27 discrete signals (12 closely spaced pairs and 3 unpaired signals), suggesting a slight break in C_2-symmetry compared to **1**. The ^1H NMR spectrum of **2** (Table 1, Figure S8) also showed an analogous pairing of similar resonances. Three secondary methyl groups were observed, evidenced by three resonances at δ_H 0.93 (d, J = 6.9 Hz; 6′-Me), δ_H 0.97 (d, J = 6.9 Hz; 6-Me) and δ_H 1.04 (d, J = 6.6 Hz; 4-Me), and two olefinic methyl groups at δ_H 1.65 (d, J = 1.3 Hz; 2′-Me) and δ_H 1.66 (d, J = 1.3 Hz; 2-Me), were observed in the ^1H NMR spectrum of **2**. The absence of a fourth secondary methyl group and its corresponding methine, and the presence of an additional methylene resonance H_2-4′ (δ_H 2.25, m), were consistent with **2** being a desmethyl analogue of **1** (Figure 1). Inspection of the $^1H - {}^1H$ COSY led to the identification of two near identical spin systems (Figure 2). Spin system A extended from H-3 to H_2-8, incorporating 4-Me and 6-Me, while spin system B extended from H-3′ to H_2-8′, incorporating 6′-Me and the methylene H_2-4′.

Identically to **1**, each spin system was found to be terminated by an α,β-unsaturated ester at one end and an oxazole motif at the other end. The ester was identified through the characteristic ^{13}C NMR chemical shifts of carbonyl carbon atoms at δ_C 165.8 (spin system A) and 165.6 (spin system B), the non-protonated olefinic carbons at δ_C 126.6 (A) and 128.0 (B) and olefinic carbons at δ_C 147.0 (A) and 142.2 (B). Diagnostic ^{1}H – ^{13}C HMBC correlations (Figure S11) from 2-Me to C-1, C-2, C-3, and from 2′ -Me to C-1′, C-2′ and C-3′, confirmed the position of the two α,β-unsaturated esters in **2**.

The oxazole motifs in **2** were characterised by the ^{13}C NMR shifts of a non-protonated carbon at δ_C 149.1 (A) and 149.2 (B), two olefinic carbons at δ_C 122.5 (A) and 122.6 (B), and a second pair of olefinic carbons at δ_C 151.2 (A) and 151.1 (B). The ^{1}H – ^{13}C HMBC correlations from H-10 to C-8, C-9 and C-11 were used to confirm the presence of oxazole motifs (Figure 2, Table S2), while the correlations from H_2-8 to C-9 and C-10, and from H_2-8′ to C-9′ and C-10′ were used to identify the location of the oxazole on the macrodiolide core. Taken together, these spectroscopic data confirmed structure **2** to be 4′-desmethylconglobatin (Figure 1). The absolute configuration of **2** was tentatively assigned to be 4*R*,6*S*,7*S*,6'*S*,7'*S* based on its close biosynthetic relationship to **1** and similar specific optical rotations (–45 for **2** vs. –58 for **1**). Interestingly, the initial structural characterisation of conglobatin was determined to be 5*S*,7*R*,8*R*,13*S*,15*R*,16*R* (equivalent to 4*S*,6*R*,7*R*,4'*S*,6'*R*,7'*R*) based on the structural similarity with vermiculin and pyrenophorin [13]. However, later synthetic studies indicated that the absolute configuration of conglobatin was in fact the opposite [30], a postulation that has been supported by recent biosynthetic studies [17].

[Figure 1]

HRESI(+)MS analysis of conglobatin C1 (**3**) indicated a molecular formula of $C_{26}H_{34}N_2O_6$ based on the protonated molecule ($[M + H]^+$ *m/z* 471.2490). An inspection of the ^{13}C spectrum of **3** revealed thirteen peaks, suggesting a symmetrical molecule. The NMR data for **3** (Table 1) were similar to those for **1**, differing only in the absence of signals for 4-Me and the substitution of the C-4 methine signals (δ_H 2.57, m; δ_C 30.7) with signals for a methylene group (δ_H 2.25, m; δ_C 24.7). Only one spin system was identified in the COSY NMR spectrum of **3** (Table S3, Figure S8), extending from H-3 to H_2-8 and incorporating 6-Me. The key ^{1}H – ^{13}C HMBC NMR correlations for **3** (Figure 3, Table S3) were the same as for **1**, confirming the presence and placement of the ester and oxazole motifs in the molecule. Based on the spectroscopic evidence, **3** was determined to be 4,4′-didesmethylconglobatin (Figure 1).

[Figure 2]

Analysis of conglobatin C2 (**4**) by HRESI(+)MS indicated the same molecular formula as **3** ($C_{26}H_{34}N_2O_6$) based on the protonated molecule ($[M + H]^+$ *m/z* 471.2482). An inspection of the ^{13}C NMR spectrum of **4** (Table 1, Figure S21) revealed twenty-six unique peaks (12 closely spaced pairs and 2 unpaired signals), indicating an asymmetric molecule. The presence of two distinct secondary methyl resonances suggested a different configuration of methyl groups on

the core. Two near-identical spin systems were identified in the $^{1}H - {}^{1}H$ COSY spectrum of **4** (Figure 3). Spin system A was found to be identical to the single spin system in **3**, while spin system B was consistent with a secondary methyl group on C-4′ instead of C-6′. The position of 4-Me was confirmed by analysis of the $^{1}H - {}^{13}C$ HMBC NMR data, which revealed diagnostic correlations from H_3-4 to C-3′, C-4′ and C-5′ (Figure 3, Table S4). The remaining NMR data for **4** were consistent with the presence of two α,β-unsaturated esters and two oxazoles, as observed in **1** – **3**. Therefore, **4** was identified as the 4,6′-didesmethylconglobatin (Figure 1).

[Table 1]

HRESI(+)MS analysis of conglobatin D1 (**5**) indicated a molecular formula $C_{25}H_{34}N_2O_6$ ([M + H]$^+$ *m/z* 457.2327) containing one carbon and two hydrogen atoms fewer than **3** and **4**. The ^{13}C NMR spectrum of **5** (Table 2, Figure S27) contained twenty-five unique signals (12 closely spaced pairs and 1 unpaired signal), indicating an asymmetrical molecule. The ^{1}H and ^{13}C NMR data for **5** were very similar to those for **3**, with the only differences being the absence of one of the secondary methyl groups and its corresponding methine, and the presence of an additional methylene group (δ_H 1.61, 1.21; δ_C 30.0; C-6′). Two discrete spin systems were identified in the $^{1}H - {}^{1}H$ COSY spectrum of **5** (Figure 4, Figure S30). Spin system A was identical to the corresponding spin system in **3**, while spin system B confirmed the absence of the 6′-Me group. The $^{1}H - {}^{13}C$ HMBC NMR data for **5** (Table S5, Figure S29) were consistent with the presence of two α,β-unsaturated esters and two oxazoles in the same arrangement as **1** – **4**. From the spectroscopic data, it was concluded that **5** was 4,4′,6′-tridesmethylconglobatin (Figure 1).

[Figure 3]

Analysis of conglobatin D2 (**6**) by HRESI(+)MS indicated a molecular formula of $C_{25}H_{34}N_2O_6$ based on the protonated molecule ([M + H]$^+$ *m/z* 457.2322), which is isomeric with **5**. The ^{13}C NMR spectrum of **5** (Figure S33) contained twenty-five unique peaks (12 closely spaced pairs and 1 unpaired signal), suggesting a lack of symmetry. Significantly, only one resonance characteristic of an olefinic methyl group was observed. The absence of 2′-Me was suggested by the upfield shift of C-2′ from δ_C 166.0 to 164.1 in the ^{13}C NMR spectrum of **6** and the presence of an additional resonance at δ_H 5.68 (dd, J = 15.8, 1.1 Hz; H-2) in the ^{1}H NMR spectrum (Table 2). Consistent with the hypothesis of a closely related yet asymmetric molecule, multiple spin systems were identified in the $^{1}H - {}^{1}H$ COSY spectrum of **6** (Figure S36). Spin system A was found to be identical to the corresponding spin systems in **3** – **5**, while spin system B showed coupling between H-2′/H-3′ and H_2-4′, consistent with the absence of a methyl group at C-2′ (Figure 4, Table S6), $^{1}H - {}^{1}H$ coupling was also identified between H-6′ and 6′-Me. The lack of contiguity was likely due to the limited amount of material available for NMR analysis. In the $^{1}H - {}^{13}C$ HMBC NMR data, correlations confirmed the presence and position of two α,β-unsaturated esters and two oxazoles, while correlations from 6′-Me to C-5′, C-6′ and C-7′ confirmed the presence of a methyl group at C-6′ on the macrodiolide core

(Table S6, Figure S35). Based on the spectroscopic evidence, it was concluded that **6** was the 2′,4,4′-tridesmethyl analogue of **1** (Figure 1).

[Figure 4]

Analysis of conglobatin E (**7**) by HRESI(+)MS indicated a molecular formula of $C_{24}H_{30}N_2O_6$ based on the protonated molecule ($[M + H]^+$ *m/z* 443.2172), which is one carbon and two hydrogens less than **5** and **6**. An inspection of the ^{13}C NMR spectrum of **7** (Table 2) revealed 12 resonances, indicating the presence of symmetry. The ^1H and ^{13}C NMR data for **7** were very similar to those for **3**, except for the absence of signals for secondary methyl group 6-Me and its corresponding methine, and the presence of an additional methylene signal (δ_H 1.55, m; δ_C 30.9; C-6). The $^1H - ^1H$ COSY NMR spectrum of **7** (Table S7, Figure S42) revealed only one spin system extending from H-3 to H_2-8, consistent with a symmetrical conglobatin analogue. Key $^1H - ^{13}C$ HMBC NMR correlations (Figure 5) confirmed the presence of the α,β-unsaturated ester and oxazole moieties, as present in **1** – **6**. Therefore, **7** was concluded to be 4,4′,6,6′-tetradesmethylconglobatin (Figure 1).

[Figure 5]

[Table 2]

Biological activities

Compound **1** is known to inhibit the proliferation of cancer cell lines, causing G2/M cell-cycle arrest, induces apoptosis and down-regulates client oncoproteins of heat shock protein Hsp90 [15, 31]. In addition to cytotoxicity, **1** exhibits *in vitro* antitrypanosomal activity against *Trypanosoma brucei brucei* GUTat 3.1 [32]. The oxazole containing diolides samroiyotmycins and elaiophylin showed antimalarial activity against *Plasmodium falciparum* [16, 33]. These studies suggest dioxazole substituted dilactone macrocycles such as conglobatin, may have further antiprotozoal and cytotoxicity activity that warrants further investigation.

[Table 3]

To explore the bioassay profile of the conglobatin family of metabolites, conglobatins **1**–**7** were evaluated for *in vitro* activity in antibacterial, antifungal, antiprotozoal and antitumour bioassays (Table 3). All conglobatins showed a degree of mammalian cell toxicity on the NS-1 cell line. Notably, **2** showed a 16-fold increase and **4** displayed a 3-fold increase in cytotoxic activity against the NS-1 cell line when compared to **1**. Interestingly, the conglobatins showed a high degree of selectivity between tumour cell line (ATCC TIB-18) over the non-tumour cell line (ATCC PCS-201). As structurally related diolides and **1** have shown antiprotozoal activity,

1–**7** were tested for antiprotozoal activity against *T. foetus* and *G. duodenalis*. However neither the parent compound nor analogues showed any activity, suggesting that **1** is selectively active against *T. brucei brucei* GUTat 3.1 [32]. Only **4** showed antibacterial activity against *B. subtilis.* None of the compounds tested had any activity up to 100 µg ml^{-1} against Gram-negative bacterium *E. coli* (ATCC 25922), the fungus *Candida. albicans* (ATCC 10231) or the monocotyledonous plant *E. tef* (teff).

Discussion

Forty-two years after the original discovery of **1**, six new analogues (**2** – **7**) have been isolated from a species of *Streptomyces* taxonomically distinct from the original conglobatin producer *Streptomyces conglobatus*. The six novel conglobatin analogues retain the same gross structural features as those described by Zhou et al. in 2015 [17], consisting of head-to-tail dimerised oxazole-containing pentaketides. Therefore, it may be hypothesised that variation in the methylation pattern is dictated by the incorporation of malonyl-CoA or methylmalonyl-CoA extender units by the AT domain of the *cong* PKS. In the biosynthesis of **1**, the AT-domain of module 3 is non-functional, leading to iteration of the previous module resulting in the 2,4,6-trimethyl product [17].

[Figure 6]

Intriguingly, **3** appears to represent the expected 'collinear' 2,6-dimethyl product. This indicates that the *cong* PKS from *Streptomyces* sp. MST-91080 contains a functioning AT domain in module 3. Compound **2** constitutes a dimer of both a 2,6-dimethyl and 2,4,6-trimethyl pentaketide demonstrating that the TE domain of the PKS is capable of dimerising different polyketide variants – this phenomenon is also required for the biosynthesis of **4**, **5** and **6**. The biosynthetic origin of the other congeners is more obscure, potentially requiring multiple skips and iterations and as such warrants further investigation. Nevertheless, the flexibility of the conglobatin synthase is remarkable and the conglobatins represent a unique example of assembly-line-generated diversity.

Acknowledgements

We thank Dr John Kalaitzis (MQ) for acquisition of NMR data and Dr Matthew McKay (MQ) for acquisition of HRMS data. Heather Lacey is the recipient of an Australian Government Research Training Program Scholarship. This research was funded, in part, by the Australian Research Council (FT130100142, FT160100233) and the Cooperative Research Centres Projects scheme (CRCPFIVE000119).

References

1 Brockmann H, Henkel W. Pikromycin, ein neues Antibiotikum aus Actinomyceten. *Naturwissenschaften* 1950; 37: 138-139.

2 Omura S. *Macrolide antibiotics: chemistry, biology, and practice*. Elsevier, 2002.

3 Kamal A, Hahn G. 106. Chaksine. Part I. *J Chem Soc* 1958: 555-557.

4 Polborn KS, W.; Connolly, J. D.; Huneck, S. Structure of the Macrocycle Bis-lactone Lepranthin from the Lichen *Arthonia impolita*; an X-Ray Analysis. *Z Naturforsch* 1995; 50b: 1111-1114.

5 Kis Z, Furger P, Sigg H. Über die Isolierung von Pyrenophorol. *Cell Mol Life Sci* 1969; 25: 123-124.

6 Fuska J, Ivanitskaya L, Horakova K, Kuhr I. The cytotoxic effects of a new antibiotic vermiculine. *J Antibiot* 1974; 27: 141-142.

7 Kind R, Zeeck A, Grabley S, Thiericke R, Zerlin M. Secondary metabolites by chemical screening. 30. Helmidiol, a new macrodiolide from *Alternaria alternata*. *J Nat Prod* 1996; 59: 539-540.

8 Kaiser H, Keller‐Schierlein W. Stoffwechselprodukte von mikroorganismen. 202. Mitteilung. Strukturaufklärung von elaiophylin: Spektroskopische untersuchungen und abbau. *Helv Chim* 1981; 64: 407-424.

9 Klassen JL, Lee SR, Thomas-Poulsen M, Beemelmanns C, Kim KH. Efomycins K and L From a Termite-Associated *Streptomyces* sp. M56 and Their Putative Biosynthetic Origin. *Front Microbiol* 2019; 10: 1739.

10 Nakakoshi M, Kimura K-I, Nakajima N, Yoshihama M, Uramoto M. SNA-4606-1, a new member of elaiophylins with enzyme inhibition activity against testosterone 5 α-reductase. *J Antibiot* 1999; 52: 175-177.

11 Yamada T, Kikuchi T, Tanaka R, Numata A. Halichoblelides B and C, potent cytotoxic macrolides from a *Streptomyces* species separated from a marine fish. *Tetrahedron Lett* 2012; 53: 2842-2846.

12 Yamada T, Minoura K, Numata A. Halichoblelide, a potent cytotoxic macrolide from a *Streptomyces* species separated from a marine fish. *Tetrahedron Lett* 2002; 43: 1721-1724.

13 Westley JW, Liu C-M, Evans RH, Blount JF. Conglobatin, a novel macrolide dilactone from *Streptomyces conglobatus* ATCC 31005. *J Antibiot* 1979; 32: 874-877.

14 Hashida J, Niitsuma M, Iwatsuki M, Mori M, Ishiyama A, Namatame M *et al*. Panowamycins A and B, new antitrypanosomal isochromans produced by *Streptomyces* sp. K07-0010. *J Antibiot* 2012; 65: 197-202.

15 Huang W, Ye M, Zhang L, Wu Q, Zhang M, Xu J *et al*. FW-04-806 inhibits proliferation and induces apoptosis in human breast cancer cells by binding to N-terminus of Hsp90 and disrupting Hsp90-Cdc37 complex formation. *Mol Cancer* 2014; 13: 150.

16 Otoguro K, Iwatsuki M, Ishiyama A, Namatame M, Nishihara-Tsukashima A, Sato S *et al*. In vitro and in vivo antiprotozoal activities of bispolides and their derivatives. *J Antibiot* 2010; 63: 275-277.

17 Zhou Y, Murphy AC, Samborskyy M, Prediger P, Dias LC, Leadlay PF. Iterative Mechanism of Macrodiolide Formation in the Anticancer Compound Conglobatin. *Chem Biol* 2015; 22: 745-754.

18 Lacey HJ, Gilchrist CL, Crombie A, Kalaitzis JA, Vuong D, Rutledge PJ *et al*. Nanangenines: drimane sesquiterpenoids as the dominant metabolite cohort of a novel Australian fungus, *Aspergillus nanangensis*. *Beilstein J Org Chem* 2019; 15: 2631-2643.

19 Lacey HJ, Vuong D, Pitt JI, Lacey E, Piggott AM. Kumbicins A–D: bis-indolyl benzenoids and benzoquinones from an Australian soil fungus, *Aspergillus kumbius*. *Aust J Chem* 2016; 69: 152-160.

20 Li H, Gilchrist CL, Lacey HJ, Crombie A, Vuong D, Pitt JI *et al*. Discovery and Heterologous Biosynthesis of the Burnettramic Acids: Rare PKS-NRPS-Derived Bolaamphiphilic Pyrrolizidinediones from an Australian Fungus, *Aspergillus burnettii*. *Org Lett* 2019; 21: 1287-1291.

21 Lacey E, Tennant S. Secondary metabolites: The focus of biodiscovery and perhaps the key to unlocking new depths in taxonomy. *Microbiol Aust* 2003; 24: 34-35.

22 Klindworth A, Pruesse E, Schweer T, Peplies J, Quast C, Horn M *et al*. Evaluation of General 16S Ribosomal RNA Gene PCR Primers for Classical and Next-Generation Sequencing-Based Diversity Studies. *Nucleic Acids Res* 2013; 41: e1.

23 Sievers F, Higgins DG. Clustal Omega, accurate alignment of very large numbers of sequences. *Multiple sequence alignment methods*. Springer, 2014, pp 105-116.

24 Labeda D, Goodfellow M, Brown R, Ward A, Lanoot B, Vanncanneyt M *et al*. Phylogenetic study of the species within the family Streptomycetaceae. *Antonie Van Leeuwenhoek* 2012; 101: 73-104.

25 Price MN, Dehal PS, Arkin AP. FastTree 2–approximately maximum-likelihood trees for large alignments. *PloS one* 2010; 5: e9490.

26 Letunic I, Bork P. Interactive Tree of Life (ITOL) v3: An Online Tool for the Display and Annotation of Phylogenetic and Other Trees. *Nucleic Acids Res* 2016; 44: W242-245.

27 Williams S, Goodfellow M, Alderson G, Wellington E, Sneath P, Sackin M. Numerical classification of *Streptomyces* and related genera. *Microbiology* 1983; 129: 1743-1813.

28 Spížek J, Málek I, Doležilová L, Vondráček M, Vaněk Z. Metabolites of *Streptomyces noursei*. *Folia Microbiol* 1965; 10: 259-262.

29 Sujarit K, Kudo T, Ohkuma M, Pathom-Aree W, Lumyong S. *Streptomyces palmae* sp. nov., isolated from oil palm (*Elaeis guineensis*) rhizosphere soil. *Int J Syst Evol Micr* 2016; 66: 3983-3988.

30 Schregenberger C, Seebach D. Synthesis and determination of the absolute configuration of the macrodiolide (+)-conglobatin. *Tetrahedron Lett* 1984; 25: 5881-5884.

31 Huang W, Wu Q-d, Zhang M, Kong Y-l, Cao P-r, Zheng W *et al*. Novel Hsp90 inhibitor FW-04-806 displays potent antitumor effects in HER2-positive breast cancer cells as a single agent or in combination with lapatinib. *Cancer Lett* 2015; 356: 862-871.

32 Hashida J, Niitsuma M, Iwatsuki M, Mori M, Ishiyama A, Namatame M *et al*. Panowamycins A and B, new antitrypanosomal isochromans produced by *Streptomyces* sp. K07-0010. *J Antibiot* 2012; 65: 197-202.

33 Dramae A, Nithithanasilp S, Choowong W, Rachtawee P, Prabpai S, Kongsaeree P *et al*. Antimalarial 20-membered macrolides from *Streptomyces* sp. BCC33756. *Tetrahedron* 2013; 69: 8205-8208.

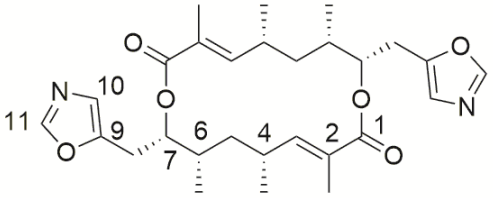

conglobatin (**1**)

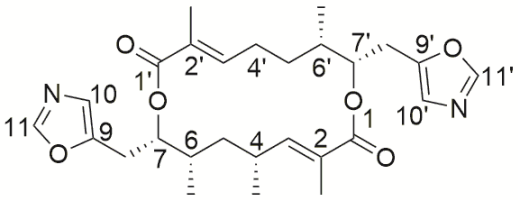

conglobatin B1 (**2**)

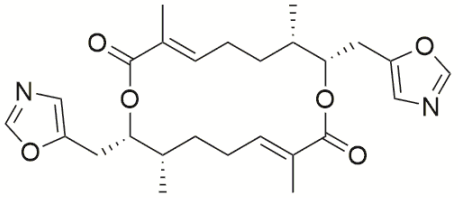

conglobatin C1 (**3**)

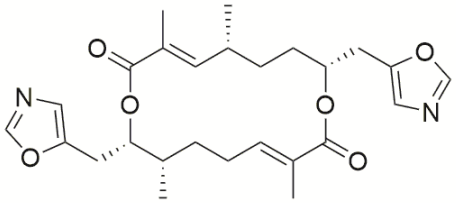

conglobatin C2 (**4**)

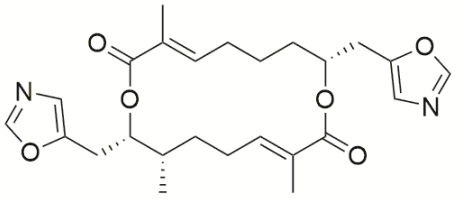

conglobatin D1 (**5**)

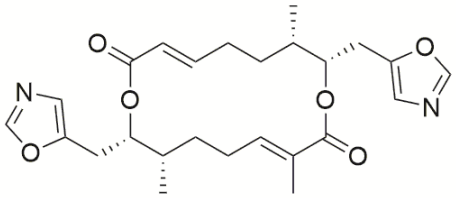

conglobatin D2 (**6**)

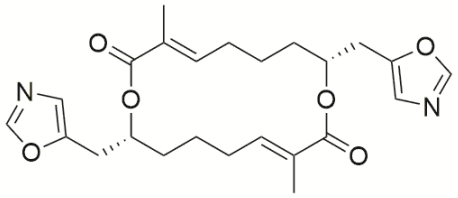

conglobatin E (**7**)

530

531 **Figure 1**. Structures of conglobatins **1**–**7** isolated from *Streptomyces* sp. MST-91080.

532

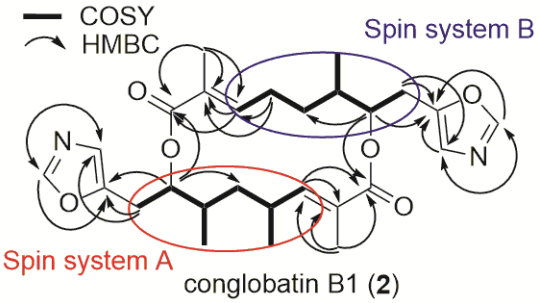

conglobatin B1 (**2**)

533

534 **Figure 2**. Selected 2D NMR correlations for conglobatin B1 (**2**).

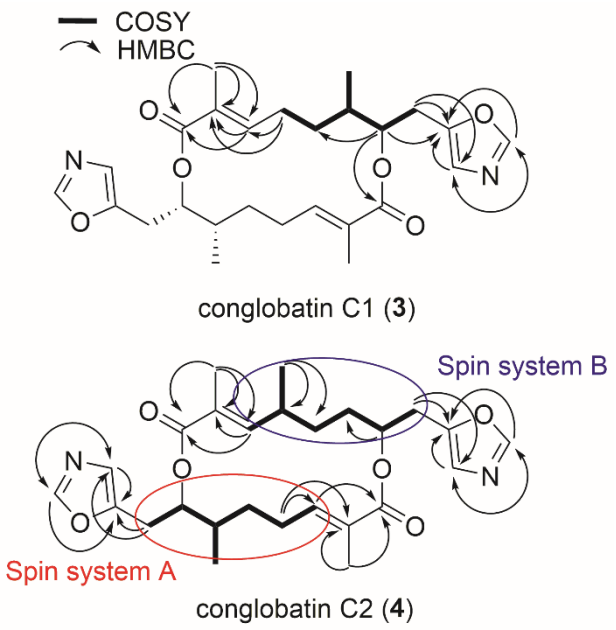

535

536 **Figure 3**. Selected 2D NMR correlations for conglobatin C1 (**3**) and conglobatin C2 (**4**).

537

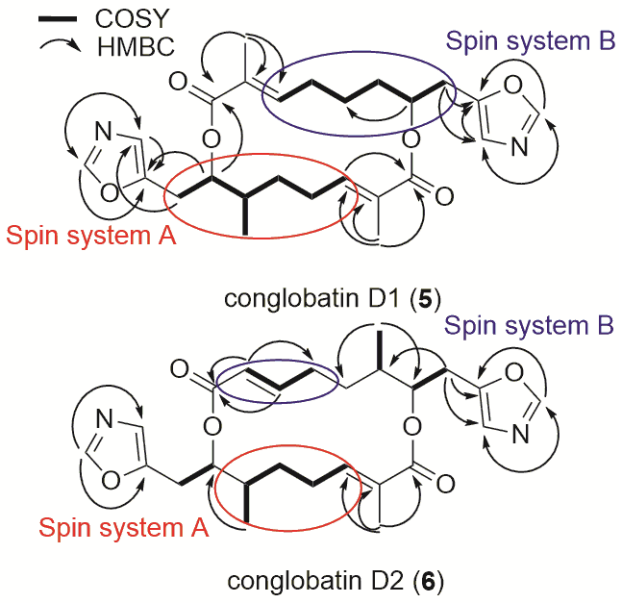

538

539 **Figure 4**. Selected 2D NMR correlations for conglobatin D1 (**5**) and conglobatin D2 (**6**).

540

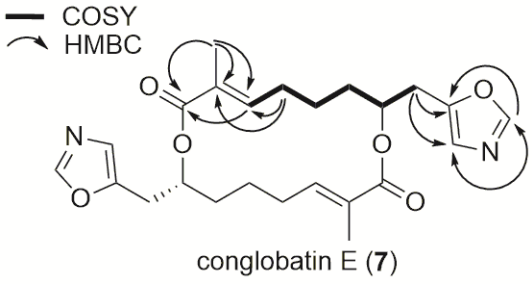

541

542 **Figure 5**. Selected 2D NMR correlations for conglobatin E (**7**).

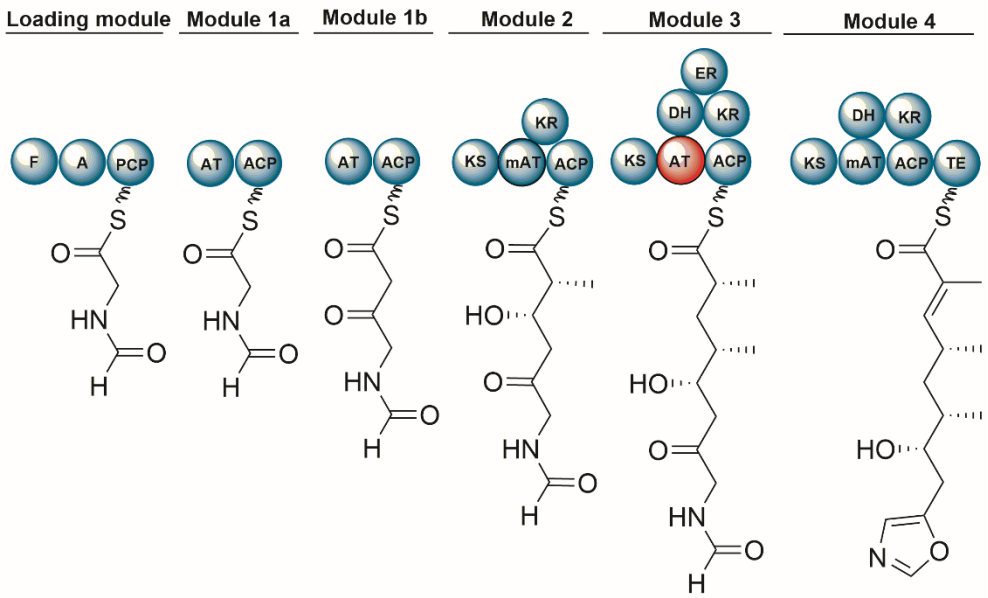

Figure 6. The putative conglobatin biosynthetic pathway adapted from [17]. Formylation (F), adenylation (A), peptidyl carrier protein-(PCP), acyltransferase (AT), acyl carrier protein (ACP), ketosynthase (KS), dehydratase (DH), enoylreductase (ER) and thioesterase (TE) domains are labelled. The inactive AT domain of module 3 is highlighted in red.

Table 1: NMR data for conglobatin (**1**), conglobatin B1 (**2**), conglobatin C1 (**3**) and conglobatin C2 (**4**) in DMSO-d_6.

	Conglobatin (**1**)		Conglobatin B1 (**2**)		Conglobatin C1 (**3**)		Conglobatin C2 (**4**)	
Pos.	δ_C	δ_H, mult. (J in Hz)	δ_C	δ_H, mult. (J in Hz)	δ_C	δ_H, mult. (J in Hz)	δ_C	δ_H, mult. (J in Hz)
1	166.0		165.8		165.6		166.1	
2	126.7		126.6		128.0		128.3	
2-Me	12.6	1.65[a], d (1.3)	12.3	1.66[a], d (1.3)	12.1	1.65, d (1.3)	12.3	1.69[a], br m
3	147.3	6.32, dd (10.4, 1.3)	147.0	6.32, dq (10.4, 1.3)	142.0	6.56, ddq (9.7, 5.8, 1.3)	142.8	6.54, dq (10.0, 1.4)
4	30.7	2.57, m	30.4	2.57, m	24.7	2.25, m	25.0	2.25, m
4-Me	21.0	1.05, d (6.5)	20.8	1.04, d (6.6)				
5	37.4	1.66[a], m	37.2	1.67[a], m	28.1	1.78, ddd (12.8, 12.0, 3.6)	28.4	1.82, dt (12.5, 3.4)
		1.25[b], m		1.25[b], m		1.39, m		1.41[b], m
6	35.0	1.26[b], m	34.6	1.26[b], m	34.4	1.32, m	35.0	1.29, m
6-Me	16.1	0.94, d (6.3)	15.7	0.97, d (6.9)	15.3	0.94, d (6.9)	15.6	0.93, d (7.0)
7	74.4	5.00, ddd (10.0, 3.0, 2.5)	74.2	4.98, ddd (10.2, 3.6, 3.0)	74.4	4.99, dd (10.3, 3.6, 3.0)	74.5	5.04, ddd (10.0, 3.6, 3.0)
8	23.9	2.97, dd (15.9, 3.0)	23.7	2.97, dd (15.9, 3.0)	23.5	2.98, dd (15.9, 3.0)	23.9	2.99, dd (15.9, 3.1)
		2.79, dd (15.9, 10.0)		2.78, dd (15.9, 10.2)		2.80, dd (15.9, 10.3)		2.82, dd (15.9, 10.0)
9	149.3		149.1		149.1		149.4	
10	122.8	6.82, s	122.5	6.82, s	122.6	6.83, s	122.8	6.82, s
11	151.3	8.19, s	151.2	8.18, s	151.1	8.19, s	151.3	8.19, s
1'			165.6				166.0	
2'			128.0				126.8	
2'-Me			12.2	1.65, d (1.3)			12.6	1.64[c], d (1.3)
3'			142.2	6.56, ddq (9.7, 5.8, 1.3)			147.2	6.36, dq (10.4 1.3)
4'			24.8	2.25, m			32.7	2.38, m
4'-Me							20.8	1.04, d (6.6)
5'			28.0	1.79, ddd (12.8, 12.0, 3.6)			29.4	1.68[a], m
				1.39, m				1.44[b], m
6'			34.5	1.25[b], m			29.7	1.64[c], m
								1.11, m
6'-Me			15.4	0.93, d (6.9)				
7'			74.3	5.03, ddd (10.1, 3.6, 3.0)			70.0	5.14, m
8'			23.6	2.98, dd (15.9, 3.0)			27.1	2.93[d], m
				2.80, dd (15.9, 10.1)				2.90[d], m
9'			149.2				148.7	
10'			122.6	6.83, s			123.1	6.92, s
11'			151.1	8.19, s			151.4	8.22, s

a-d Overlapping resonances

554

555 **Table 2:** NMR data for conglobatin D1 (**5**), conglobatin D2 (**6**) and conglobatin E (**7**) in DMSO-d_6.

	Conglobatin D1 (**5**)		Conglobatin D2 (**6**)		Conglobatin E (**7**)	
Pos.	δ_C	δ_H, mult. (*J* in Hz)	δ_C	δ_H, mult. (*J* in Hz)	δ_C	δ_H, mult. (*J* in Hz)
1	166.1		166.0		166.3	
2	128.3		128.3		127.7	
2-Me	12.3	1.69, s	12.4	1.67, s	12.3	1.69, s
3	142.5	6.55, dq (8.8, 1.4)	142.1	6.54, dq (9.2, 1.3)	142.1	6.66, dq (9.2, 1.3)
4	24.9	2.25[a], m	24.9	2.25, m	26.5	2.17, m
						2.12, m
5	28.5	1.79[b], m	28.3[g]	1.77, m	22.0	1.64, m
		1.41[c], m		1.38[a], m		1.42, m
6	34.7	1.38[c], m	34.5	1.39[a], m	30.9	1.55, m
6-Me	15.6	0.94, d (6.6)	15.8	0.95, d (6.4)		
7	74.7	4.99, ddd (10.2, 3.0, 2.7)	74.4	4.98[b], dm (10.3)	71.0	4.99, dddd (6.9, 6.5, 6.5, 3.2)
8	23.9	2.98, dd (15.8, 3.0)	23.6	2.97[c], dm (15.8)	28.8	2.97, d (6.5)
		2.81, dd (15.8, 10.2)		2.81[d], dt (15.8, 10.3)	148.6	
9	149.3		149.4		123.3	6.91, s
10	122.9	6.83, s	122.8	6.84[e], s	151.5	8.23, s
11	151.2	8.19, s	151.3	8.19[f], s		
1'	166.0		164.1			
2'	128.2		122.6	5.68, dd (15.8, 1.1)		
2'-Me	12.3	1.64[d], s				
3'	142.3	6.58, dq (10.5, 1.4)	149.5	6.74, ddd (15.8, 9.7, 5.2)		
4'	26.8	2.26[a], m	28.2	2.37, m		
		2.09, m		2.07, m		
5'	20.6	1.81[b], m	28.0	1.74, m		
		1.56, m		1.38[a], m		
6'	30.0	1.61[d], m	33.5	1.49, m		
		1.21, m				
6'-Me			15.8	0.94, d (7.0)		
7'	70.3	5.13, m	74.9	4.98[b], dm (10.3)		
8'	27.3	2.95, br d (3.5)	23.8	2.98[c], dm (15.8)		
		2.94, br d (2.7)		2.81[d], td (15.8, 10.3)		
9'	148.7		149.4			
10'	123.1	6.91, s	122.9	6.84[e], s		
11'	151.4	8.22, s	151.3	8.19[f], s		

556 a-f Overlapping resonances

557

Table 3. *In vitro* bioassay data for **1** – **7**.

Compound	IC_{50} (µg ml^{-1})		
	NS-1[c]	Nff[d]	Bs[e]
1[a]	1.39 ± 0.09	>100	>100
2[a]	0.084 ± 0.009	>100	>100
3[a]	1.05 ± 0.04	>100	>100
4[a]	0.45 ± 0.04	>100	73.3 ± 1.4
5[a]	17.8 ± 1.2	>100	>100
6[b]	12.5	50.0	>100
7[b]	25.0	100.0	>100
Control	0.02[f]	0.2[f]	0.2[g]

[a] Experiments were conducted in triplicate. IC_{50} values are mean ± standard error; [b] Only one experiment was conducted [c] Mouse myeloma NS-1 cell line (ATCC TIB-18); [d] Human fibroblast NFF cell line (ATCC PCS-201); [e] *Bacillus subtilis* (ATCC 6633); [f] doxorubicin; [g] Amoxicillin.